Journal of Orthopaedic Surgery and Research

RESEARCH

Open Access

Decreased serum and local GPX4 and SLC7A11 expression correlates with disease severity in non-traumatic osteonecrosis of the femoral head

Qing-He Ye[1,2], Peng Zhang[1,2], Yong-Heng Zhao[1,2], Wen-Xiu Zhu[1,2], Hong-Xun Zhu[1,2] and Biao-Fang Wei[2*]

Abstract

Background Ferroptosis is implicated in various musculoskeletal conditions, including non-traumatic osteonecrosis of the femoral head (NT-ONFH).

Objective The objective of this study was to explore the levels of two crucial proteins associated with ferroptosis, namely Glutathione peroxidase 4 (GPX4) and Solute Carrier Family 7 Member 11 (SLC7A11), in both serum and femoral head samples, and to correlate their expression levels with the clinical severity of NT-ONFH.

Methods The study included 136 NT-ONFH patients and an equal number of healthy controls. In addition, 68 subjects suffering from femoral neck fractures (FNF) were included in the study. The serum concentrations of GPX4 and SLC7A11 were quantified using the enzyme-linked immunosorbent assay. The GPX4 and SLC7A11 levels among tissue samples were identified through immunohistochemical staining, western blot analysis, and quantitative real-time polymerase chain reaction (qRT-PCR). The radiographic severity of the condition was evaluated utilizing the Association Research Circulation Osseous (ARCO) classification system, while the symptomatic severity was assessed utilizing the Visual Analogue Scale (VAS) alongside the Harris Hip Score (HHS).

Results Patients diagnosed with NT-ONFH had considerably reduced serum concentrations of GPX4 and SLC7A11 in comparison to individuals in the healthy control group. Negative correlations of serum GPX4 and SLC7A11 levels with the ARCO stages were observed. A total of 73 ONFH and 68 FNF patients underwent total hip replacement. The mRNA and protein levels of GPX4 and SLC7A11 were lower in the necrotic areas compared to the non-necrotic areas and FNF femoral head tissues. Subsequent Receiver operating characteristic (ROC) curve analysis suggested that the decreased levels of both serum and local GPX4 and SLC7A11 could serve as potential biomarkers for the progression of ONFH. Furthermore, serum and local GPX4 and SLC7A11 levels were found to be negatively linked to the VAS score but positively related to the HHS score.

*Correspondence:
Biao-Fang Wei
weibf2022@163.com

Full list of author information is available at the end of the article

Conclusion The levels of GPX4 and SLC7A11, both in serum and at the local site, were inversely correlated with the progression of NT-ONFH. Targeting ferroptosis and its associated proteins through potential therapeutic interventions could be a viable strategy to mitigate the severity of NT-ONFH.

Keywords Non-traumatic osteonecrosis of femoral head, Glutathione peroxidase 4, Solute carrier family 7 member 11, Disease severity

Introduction

As a debilitating bone disorder, non-traumatic osteonecrosis of the femoral head (NT-ONFH) is marked by the malfunctioning of the femoral head's microvasculature as well as disruptions in bone metabolism [1, 2]. Among various NT-ONFH cases, those caused by steroids are the most frequent, with alcohol-induced cases coming next, and then those linked to other factors such as blood disorders, genetic predispositions, or of unknown causes [3, 4]. It is predicted that the worldwide count of ONFH patients could hit 20 million within ten years.This condition often leads to profound functional limitations and can cause disability, placing a considerable financial strain on the affected individuals, their households, and society in general [5]. The misuse of steroids and excessive alcohol consumption are established risk factors for ONFH, as they can trigger issues with lipid metabolism, diminish the capacity for bone formation, hinder blood circulation, incite inflammation, and induce cell death, all of which could contribute to ONFH [6, 7]. Moreover, steriods and alcohol are known to encourage the transformation of mesenchymal stem cells into fat cells [8].

Ferroptosis differs from other forms of programmed cell death in the context of morphology, genetic mechanisms, as well as biochemical processes [9]. It is marked by the accumulation of iron and reactive oxygen species (ROS) within the cells, inhibition of the cystine-glutamate antiporter system X_c^-, reduction in glutathione levels, oxidation of nicotinamide adenine dinucleotide phosphate (NADPH), and lipid peroxidation [9]. Research has demonstrated that ferroptosis has a substantial impact on the pathology of a wide range of illnesses, including but not limited to cancer [10], cardiovascular diseases [11], neurological disorders [12], rheumatic diseases [13], musculoskeletal conditions [14], and diabetes [15].

At the molecular level, ferroptosis is triggered by the inhibition of glutathione peroxidase 4 (GPX4), a key enzyme involved in maintaining cellular redox homeostasis. GPX4 plays an essential role in neutralizing ROS by reducing lipid hydroperoxides to their corresponding alcohols [16]. A decrease in GPX4 activity can stem from either direct inhibition of its enzymatic function or from enhanced degradation by certain inducers [17]. The impairment or absence of GPX4 activity directly activates ferroptosis due to the subsequent buildup of lipid peroxides [18]. Solute Carrier Family 7 Member 11 (SLC7A11) constitutes the light chain of the cystine/glutamate antiporter system X_c^-, and it plays an essential role in maintaining the redox equilibrium within cells [19]. When system X_c^- is compromised, the cellular levels of cysteine are diminished, which subsequently hinders the production of glutathione (GSH) alongside GPX4's activity, ultimately initiating ferroptosis [20].

Ferroptosis has been demonstrated to be involved in the progression of NT-ONFH. Dexamethasone is capable of inhibiting the expression of SLC7A11 and GPX4, which results in a decrease in the intracellular levels of GSH and a concurrent rise in the levels of malondialdehyde and ROS [21]. This suppression also results in a decrease in mitochondrial size and cristae, which are hallmark features of ferroptosis. Elevating the SLC7A11 level or employing a ferroptosis inhibitor like Ferrostatin-1 could mitigate ferroptosis triggered by dexamethasone in MC3T3-E1 cells. This indicates that dexamethasone triggers ferroptosis in MC3T3-E1 cells through the activation of the p53/SLC7A11/GPX4 signaling pathway [21].

Steriods and alcohol has been proved to facilitate ferroptosis from different aspects.For example, Dexamethasone could sensitize ferroptosis by glucocorticoid receptor–induced dipeptidase-1 expression and glutathione depletion [22]. Dexamethasone -induced osteoporosis is tightly related to the ferroptosis and deceased GPX/SLC7A11 expressions [23].On the other hand, alcohol could induced hepatocyte iron death, accompanied by accumulation of lipid peroxidation and decreased expression of SLC7A11 and GPX4 [24].In another study, alvohol could induce rat liver injury model, and inhibition of p62/Nrf2/Keap1/SLC7A11 pathway by fucoidan could protect hepatocytes from ferroptosis and inhibit iron overload [25].

The objective of this study was to establish a link between the concentrations of GPX4 and SLC7A11, in both serum and local tissues, and the advancement of NT-ONFH patients.

Patients and methods

Study patients

The study enrolled a total of 136 patients with NT-ONFH at Linyi People's Hospital in Shandong Province, China, from October 2023 to September 2024. Out of these 136 patients, 70 had NT-ONFH due to steroid use and 66 due to alcohol consumption, as determined by their medical histories. The inclusion criteria for steroid-related

ONFH were: (1) patients with a record of corticosteroid consumption exceeding cumulative dose of 2 g of prednisolone or an equivalent dose within 3 months; (2) patients diagnosed with osteonecrosis within 2 years post-corticosteroid treatment; and (3) patients without other risk factors besides corticosteroid use [26]. The inclusion criteria for alcohol-related ONFH were: (1) patients with documented weekly alcohol consumption exceeding 400 mL, equivalent to 320 g of pure ethanol, for a period exceeding six months; (2) patients with diagnosis of ONFH within one year following the specified alcohol intake; and (3) patients with no other risk factors present apart from alcohol misuse [27]. Individuals were excluded from the study in case that they had a medical history of metabolic or endocrine disorders, chronic diseases, cancer, prior glucocorticoid or chemotherapy treatments, or if they were taking medications known to affect bone metabolism. Concurrently, 136 healthy individuals were recruited as controls, who were selected based on the absence of hip pain and normal findings on anteroposterior and frog leg lateral pelvic radiographs, with no signs of sclerotic margins or subchondral collapse indicative of ONFH.

Out of the 136 patients diagnosed with NT-ONFH, 33 who were at Association Research Circulation Osseous (ARCO) stage 4 as well as 35 patients at ARCO stage 3 received total hip replacement (THR). Concurrently, 36 patients with femoral neck fracture (FNF) who underwent THR were incorporated as a control group. All femoral head tissues from FNF patients did not show necrotic manifestations.Tissue samples from the femoral head were collected for subsequent analysis.

The study was approved by the Regional Committee for Science and Research Ethics at Linyi People's Hospital (Approval No. 20230030). All participants involved in the study signed written informed consent.

Western blotting

Briefly, the bone tissue samples were first placed into a mortar containing liquid nitrogen and crushed into a fine powder. The powdered bone tissue was then transferred to an Eppendorf (EP) tube (1.5 mL) and mixed with protein lysate. The samples were lysed using ristocetin-induced platelet aggregation (RIPA) buffer (Beyotime, China). The protein samples, once denatured (20 μg per lane), were subjected to separation via a 10% SDS-polyacrylamide gel electrophoresis (SDS-PAGE) gel and subsequently transferred onto polyvinylidene fluoride (PVDF) membranes from EMD Millipore, USA. The primary antibodies applied were as follows: GPX4 (1:1000, ab125066; Abcam, UK), SLC7A11 (1:1000, ab307601; Abcam, UK), together with GAPDH (1:3000, ab8226; Abcam, UK). To detect protein bands, horseradish peroxidase-conjugated secondary antibodies were used, and the visualization of blots were achieved through the Clarity Western ECL Substrate Kit (Bio-Rad, USA).

Immunohistochemistry (IHC)

The IHC assay was performed following standard procedures. Tissues from patients with NT-ONFH and FNF were sectioned into paraffin-embedded slices approximately 5 micrometers thick. The sections underwent a series of preparatory steps including the removal of paraffin, rehydration, and blocking. Subsequently, they were incubated with primary antibodies against GPX4 (1:1000, Abcam, UK) as well as human SLC7A11 (1:1000, Abcam, UK), followed by an incubation at the temperature of 37 °C for one hour. Subsequently, a secondary antibody, Rabbit anti-human IgG (1:1000), was applied for a 20-minute blocking period. The expression of the proteins in the tissues was then examined using a fluorescence microscope (Olympus, Tokyo, Japan). The histochemical score for each tissue sample was determined by multiplying the percentage of positively stained area by the intensity of the staining, with the calculation facilitated by ImageJ software.

Quantitative reverse transcription polymerase chain reaction (qRT-PCR)

The mRNA levels of GPX4 and SLC7A11 were determined through RT-qPCR, utilizing SYBR Green as a fluorescent marker. Each sample was subjected to RT-qPCR three times to ensure accuracy. The relative gene expression levels were computed utilizing the $2^{-\Delta\Delta CT}$ method. The specific primer sequences used for amplification are as follows: (1) GPX4: Forward: 5'-AGAGATCAAAGAGT TCGCCGC-3', Reverse: 5'-TCTTCATCCACTTCCACA GCG-3'; (2) SLC7A11: Forward: 5'-GCTGTGATATCCC TGGCATT-3', Reverse: 5'-GGCGTCTTTAAAGTTCTG CG-3'; (3) GAPDH: Forward: 5'-TGTGTCCGTCGTGG ATCTGA-3', Reverse: 5'-CCTGCTTCACCACCTTCTT GA-3′.

Enzyme-Linked Immunosorbent Assay (ELISA)

Blood samples were drawn from the elbow vein in the morning while subjects were fasting, and the samples were collected into tubes with an procoagulant. Following a 2-hour incubation period, the blood samples underwent centrifugation at 3,000 g for a period of 15 min at the temperature of 4°C to facilitate the separation of serum from the cellular components. Subsequently, the levels of SLC7A11 (item number: SEE410Hu, supplied by Cloud-clone Inc., based in Katy, Texas) and GPX4 (item number: SEE994Hu, also from Cloud-clone Inc.) in the serum were quantified utilizing ELISA kits (R&D Systems, Inc., Minneapolis, Minnesota), strictly in accordance with the guidelines supplied by the manufacturer. Next, their absorbance was quantified at the wavelength

of 450 nm utilizing a microplate reader. The assays are capable of detecting SLC7A11 at concentrations ranging from 0.156 to 10 ng/mL, while GPX4 can be detected within a range of 3.12 to 200 ng/mL. Each dataset was derived from three separate experiments to ensure reliability. The intra-assay variation coefficients were 6.8% for SLC7A11 and 8.8% for GPX4, while the inter-assay variation coefficients were 7.5% for SLC7A11 and 9.3% for GPX4.

Radiological evaluation

The radiographic assessments were conducted using the ARCO classification system for ONFH, which is based on the characteristics observed through X-ray and MRI [8]. The ACRO classification system, is outlined below: (1) Stage 0 indicates that there are no abnormalities observed in diagnostic imaging; (2) Stage 1 signifies that conventional radiography and CT scans appear normal, but MRI or scintigraphy, or a combination of both, detect osteonecrosis; (3) Stage 2 is characterized by radiographic evidence of irregularities such as mottling, osteolysis, and sclerosis, but the femoral head retains a spherical appearance on anteroposterior and lateral projections; (4) Stage 3 is marked by the presence of the "crescent sign" on radiographs, a thin radiolucent line suggesting subchondral fracture, coinciding with mechanical collapse of the femoral head; (5) Stage 4 is identified by the obvious flattening of the femoral head, a reduction in the joint space, and alterations in the acetabulum. The study enrolled patients with ONFH who were classified at ARCO stages 2 or higher. When both hips were influenced, the more severely impacted side was chosen for study evaluation.

Assessment of clinical severity

Clinical severity of the patients was evaluated utilizing the Visual Analogue Scale (VAS) together with Harris Hip Score (HHS). As a pain measurement instrument, the VAS employed a 10 cm long line, with one end marked "0" indicating the absence of pain and the opposite end marked "10" representing the most severe pain that can be imagined, allowing patients to mark their own pain level [28].VAS scores of 0–3, 4–6, and 7–10 points were indicative of mild, moderate, and severe pain, respectively. The HHS, introduced by Harris in 1969, could evaluate the functional outcomes and surgical efficacy for patients who have undergone hip replacement surgery [29]. This scoring system had a maximum possible score of 100 points, with assessment criteria focusing on pain, functionality, deformities, as well as mobility. The HHS categorized results into four performance levels based on the total score. Specifically, scores of 90–100, 80–89, 70–79, and <69 corresponded to excellent, good, fair, and poor levels, respectively.

Statistical analysis

Data followed normal distribution based on Shapiro-Wilk test, and were described with the mean ± standard deviation (SD) derived from separate experimental trials. For comparison between two groups, Student's t-test was employed to compare the mean expressions of gene or proteins. When comparing parameters across ≥ 3 groups, one-way analysis of variance (ANOVA) was conducted, which was then supplemented by the Bonferroni post-hoc test for multiple comparisons to analyze specific differences between groups. GraphPad Prism 8.0 was used for data analysis. The diagnostic efficacy of GPX4 alongside SLC7A11 within the ARCO grading system was assessed utilizing receiver operating characteristic (ROC) curves. The possible associations of GPX4 and SLC7A11 with various other factors were assessed utilizing either Spearman's or Pearson's correlation methods. The statistical significance threshold was established at a p-value threshold of less than 0.05.

Results

Demographic information

Patients with NT-ONFH included 71 male and 65 female individuals, with the average age of 53.1 ± 7.1 years (range:38–66 years); while the control group comprised 69 males together with 67 females, and the mean age was 52.4 ± 6.8 years old (range:37–65 years old). Regarding of the body mass index (BMI), the average value for individuals with NT-ONFH was 23.5 ± 2.2 kg/m^2, while for healthy controls (HCs), it was 23.0 ± 2.6 kg/m^2.m The gender ($P = 0.703$), age ($P = 0.242$), alongside BMI ($P = 0.327$) did not show any significant difference between groups, as summarized in Table 1.

Local GPX4 and SLC7A11 expressions in femoral head tissues

GPX4 and SLC7A11 levels within tissues from the femoral heads of individuals with NT-ONFH were investigated. The mRNA and protein levels of GPX4 and SLC7A11 were considerably lower within the necrotic areas (NA) of the femoral head in contrast with those within the non-necrotic areas (NNA) and the FNF control group (Figs. 1A-B and 2A-D). IHC analysis revealed significantly lower levels of GPX4 and SLC7A11 proteins in the NA group compared to both the NNA group and the FNF control group, as depicted in Fig. 3A and B. For the semi-quantitative evaluation of GPX4 and SLC7A11 expression, the integrated optical density (IOD) values were measured utilizing Image-Pro Plus software. The average IOD values for GPX4 and SLC7A11 were 0.13 ± 0.02 and 0.14 ± 0.02 for the NA group, 0.62 ± 0.02 and 0.63 ± 0.02 for the NNA group, and 0.63 ± 0.02 and 0.65 ± 0.02 for the FNF control group, respectively (Fig. 4A, B).These results indicated significant differences

Table 1 Demographic information of study participants

	NT-ONFH patients ($n=136$)	Healthy controls ($n=136$)	*P* value
Age (Y)	53.1 ± 7.1	51.2 ± 6.2	0.242
Gender (F/M)	65/71	67/69	0.703
BMI	23.5 ± 2.2	23.0 ± 2.6	0.327
VAS score	4.7 ± 1.5	/	
HHS score	61.0 ± 7.8	/	
ARCO stage (2/3/4)	45/47/44	/	
Etiology			
Steriod/Alcoholic	70/66	/	
Serum GPX4 Levels (ng/mL)	13.02 ± 2.35	18.05 ± 3.30	< 0.001
Serum SLC7A11 Levels (ng/mL)	3.57 ± 1.15	5.52 ± 1.61	< 0.001

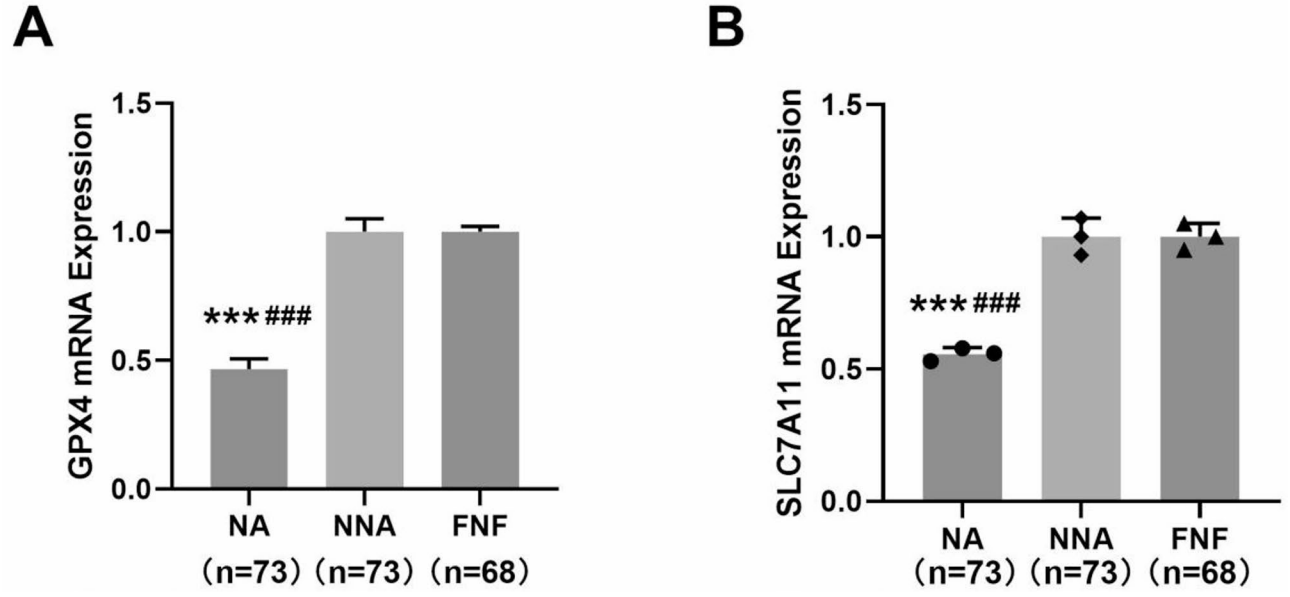

Fig. 1 (**A**) Comparison of GPX4 mRNA expression among the NA, NNA, alongside FNF groups. (**B**) Comparison of SLC7A11 expression among the NA, NNA, alongside FNF groups. NA: Necrotic Area; NNA: Non-necrotic Area; FNF: Femoral Neck Fracture.$^{***}P < 0.001$ vs. NNA; $^{\#\#\#}P < 0.001$ vs. FNF

in GPX4 and SLC7A11 protein expression in the comparison of the NA group with either the NNA group or the FNF control group.

Serum GPX4 and SLC7A11 levels in NT-ONFH patients

Figure 4 illustrates that in contrast with HCs, individuals with NT-ONFH had lower concentrations of GPX4 (13.02 ± 2.35 ng/mL versus 18.05 ± 3.30 ng/mL) and SLC7A11 (SLC7A11: 3.57 ± 1.15 ng/mL versus 5.52 ± 1.61 ng/mL) (both $P < 0.001$), as depicted in Fig. 4A and B. Based on the etiology of NT-ONFH, participants in the study were classified into two groups: those with NT-ONFH due to steroid use (70 cases) and those with NT-ONFH due to alcohol consumption (66 cases). Nevertheless, the serum concentrations of GPX4 (13.025 ± 2.37 ng/mL versus 12.78 ± 2.32 ng/mL) and SLC7A11 (3.50 ± 1.17 ng/mL versus 3.64 ± 1.14 ng/mL) did not show any significant differences between the ONFH patients induced by steroid and alcohol (both $P > 0.05$), as illustrated in Fig. 4C and D.

Serum GPX4 and SLC7A11 levels among different ARCO stages in ONFH patients

Table 1 details the serum levels of GPX4 and SLC7A11 for patients with NT-ONFH across various ARCO stages. The 136 ONFH patients were categorized according to their ARCO stages into 45 patients in grade 2, 47 in grade 3, and 44 in grade 4.

Compared to those at ARCO stage 3, individuals with NT-ONFH at ARCO stage 2 exhibited significantly higher serum levels of GPX4 (14.26 ± 1.90 ng/mL versus 13.05 ± 2.41 ng/mL, $P = 0.009$) and SLC7A11 (4.22 ± 0.93 ng/mL versus 3.66 ± 1.19 ng/mL, $P = 0.013$), as illustrated in Fig. 5A and B. Furthermore, patients with NT-ONFH at ARCO stage 3 had considerably higher serum GPX4 level (13.05 ± 2.41 ng/mL versus 11.72 ± 2.02 ng/mL, $P = 0.005$) and serum SLC7A11 (3.66 ± 1.19 ng/mL

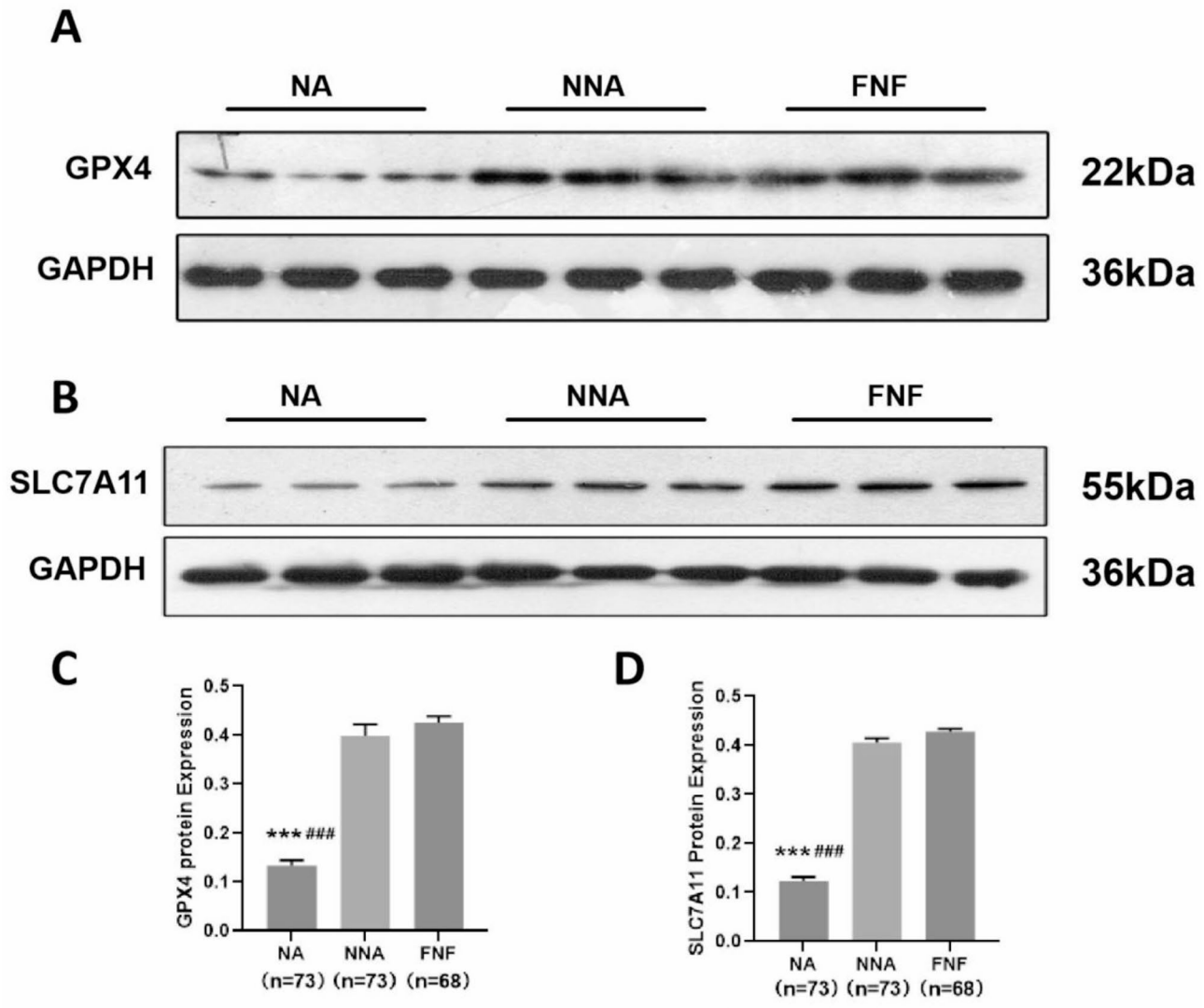

Fig. 2 (**A**) Representative Western blots of GPX4 protein bands among the NA, NNA and FNF groups. (**B**) Representative Western blots of SLC7A11 protein bands among the NA, NNA and FNF groups. (**C**) Analysis of GPX4 protein expression among the NA, NNA and FNF groups. (**D**) Analysis of SLC7A11 protein expression among the NA, NNA and FNF groups. NA: Necrotic Area; NNA: Non-necrotic Area; FNF: Femoral Neck Fracture. ***$P < 0.001$ vs. NNA; ###$P < 0.001$ vs. FNF

versus 2.81 ± 0.84 ng/mL, $P < 0.001$) level than those at ARCO stage 4, as shown in Fig. 5A and B. Figure 5C and D demonstrate negative correlations of serum GPX4 level (r = -0.439) and serum SLC7A11 level (r = -0.498) with ARCO stages (both $P < 0.001$).

ROC curve analysis

The area under the curve (AUC) values for serum levels of GPX4 were significant different when comparing ARCO stage 2 to stage 3 (AUC = 0.645, $P = 0.017$) and when comparing ARCO stage 3 to stage 4 (AUC = 0.659, $P = 0.009$) (Fig. 6A, B). Similarly, the serum levels of SLC7A11 had significant AUC values for the comparison between ARCO stage 2 and stage 3 (AUC = 0.637, $P = 0.024$), as well as between ARCO stage 3 and stage 4 (AUC = 0.713, $P < 0.001$) (Fig. 6C, D). Our findings suggest that reduced levels of serum GPX4 and SLC7A11 could potentially be used as diagnostic indicators for NT-ONFH across its varying stages.

Correlation of serum GPX4 and SLC7A11 concentrations with clinical outcomes

The study investigated the correlation of serum GPX4 and SLC7A11 levels with the clinical severity of patients suffering from NT-ONFH. Serum GPX4 level (r = -0.422) and serum SLC7A11 level (r = -0.437) were negatively correlated with VAS scores, indicating an inverse relationship with pain severity (both $P < 0.001$), as depicted in Fig. 7A and B. Additionally, serum GPX4 level ($r = 0.450$), and serum SLC7A11 level ($r = 0.454$) were positively

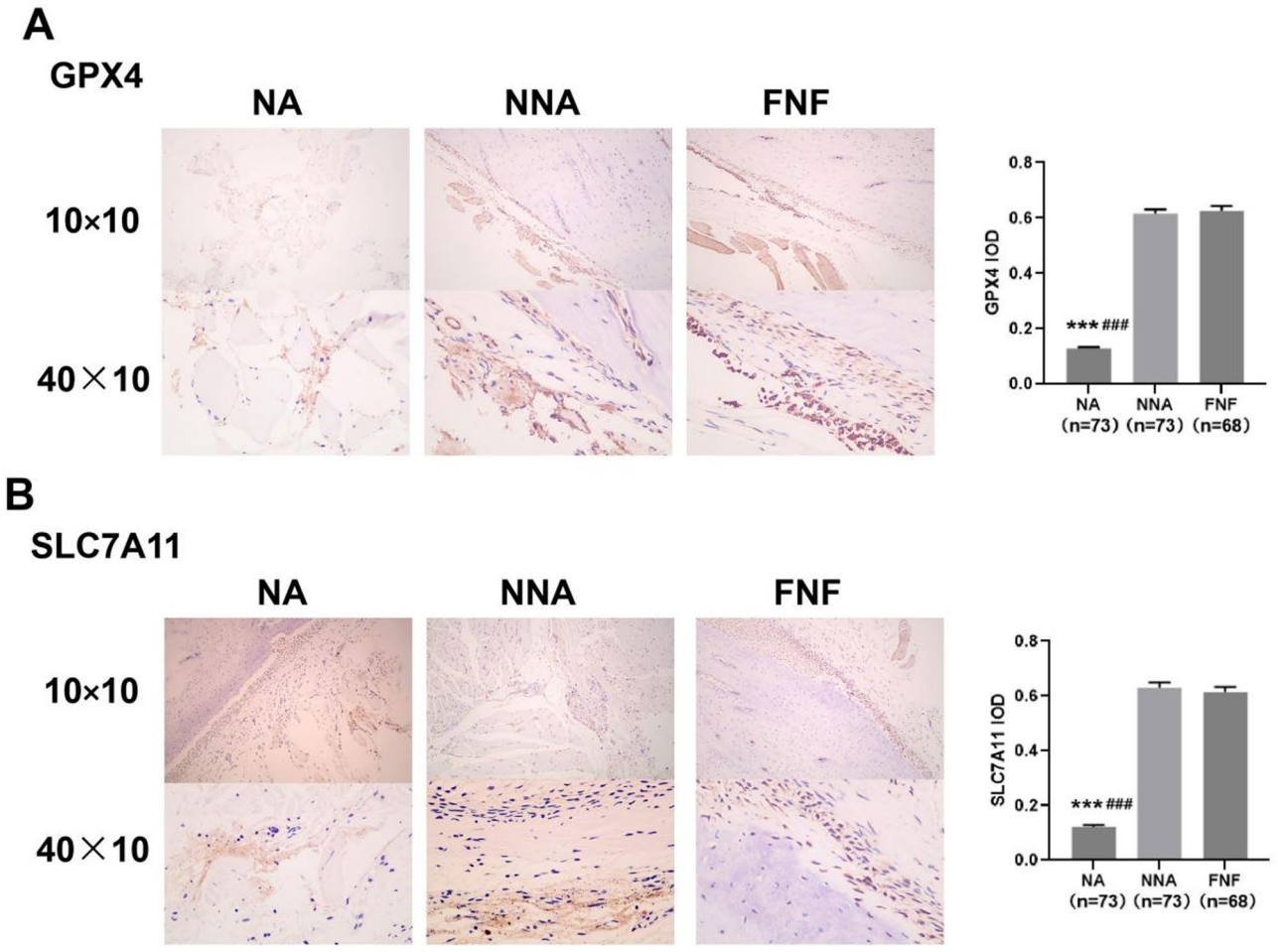

Fig. 3 (**A**) Comparison of local protein expression among the NA, NNA and FNF groups. (**B**) Comparison of local SLC7A11 protein expression among the NA, NNA and FNF groups. NA: Necrotic Area; NNA: Non-necrotic Area; FNF: Femoral Neck Fracture.$^{***}P<0.001$ vs. NNA; $^{###}P<0.001$ vs. FNF

linked to the HHS (both $P<0.001$), suggesting a direct relationship with better functional outcomes, as shown in Fig. 7C and D.

Discussion

Ferroptosis is linked to the advancement of ONFH. In a study [30], thirty samples of osteonecrosis triggered by steroid use and ten samples of osteonecrosis not related to steroids were collected from the Gene Expression Omnibus (GEO) database. Differentially expressed genes (DEGs) between groups were identified. Genes related to ferroptosis were acquired from the Ferroptosis Database (FerrDb). By intersecting the ferroptosis-related genes with the DEGs, ferroptosis-related DEGs were identified. Subsequently, KEGG and GO enrichment analyses were carried out to investigate the ferroptosis-related DEGs. This approach validated the ferroptosis-associated genes and pathways in the progression of steroid-induced osteonecrosis, shedding light on ferroptosis's impact on femoral head necrosis.

Our study initially revealed decreased expressions of GPX4 and SLC7A11 among patients with NT-ONFH. This finding aligned with the findings from various studies that have documented lower levels of these proteins in a range of bone and rheumatic diseases, including osteoarthritis [31, 32], rheumatoid arthritis [13], and osteoporosis [33, 34]. Furthermore, we discovered a correlation between the downregulation of GPX4 and SLC7A11 and the progression of ONFH. This is supported by evidence showing that the suppression of the SLC7A11/GPX4 pathway can induce ferroptosis in osteoblasts, exerting a pivotal impact on the occurrence of osteoblastic death, resulting in ONFH [35]. Additionally, we found that elevated serum levels of SLC7A11 and GPX4 were linked to reduced pain and improved functionality, showing a positive correlation. This relationship is particularly evident in neuropathic, inflammatory, and cancer-related pain, where the disruption of ferroptosis and the associated changes in GPX4 and SLC7A11 levels are key contributors [36]. We also noticed that GPX4 and SLC7A11 levels did not differ between steriod and alcoholic induced

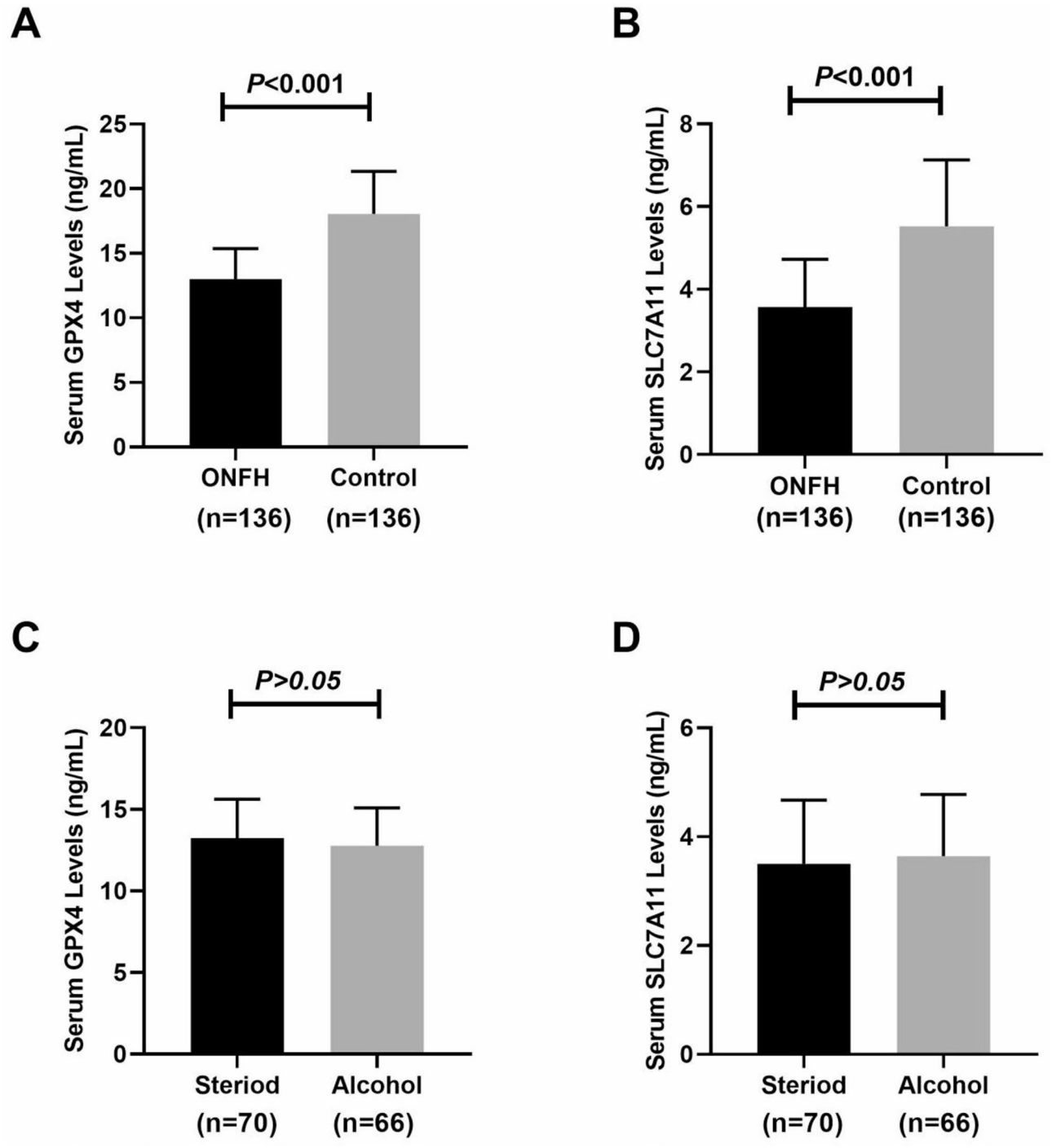

Fig. 4 (**A**) Analysis of serum GPX4 levels between ONFH and controls (**B**) Analysis of serum SLC7A11 levels between ONFH and controls. (**C**) Analysis of serum GPX4 levels between individuals with NT-ONFH due to steroid use and those with NT-ONFH due to alcohol consumption. (**D**) Analysis of serum SLC7A11 levels between individuals with NT-ONFH due to steroid use and those with NT-ONFH due to alcohol consumption

ONFH patients.Steriod and alcohol may both affect GPX4 and SLC7A11 expressions through the same pathway signaling. Steriod and alcohol can both decrease the expressions of GPX4 and SLC7A11 in different conditions [37, 38].

The family of GPX, especially GPX4, is involved in neutralizing oxidative stress and preserving the cellular redox equilibrium. GPX4 can prevent ferroptosis and alleviate diverse pain conditions. In the context of inflammation, the generation of substantial ROS as well as reactive nitrogen species (RNS) can result in direct tissue damage

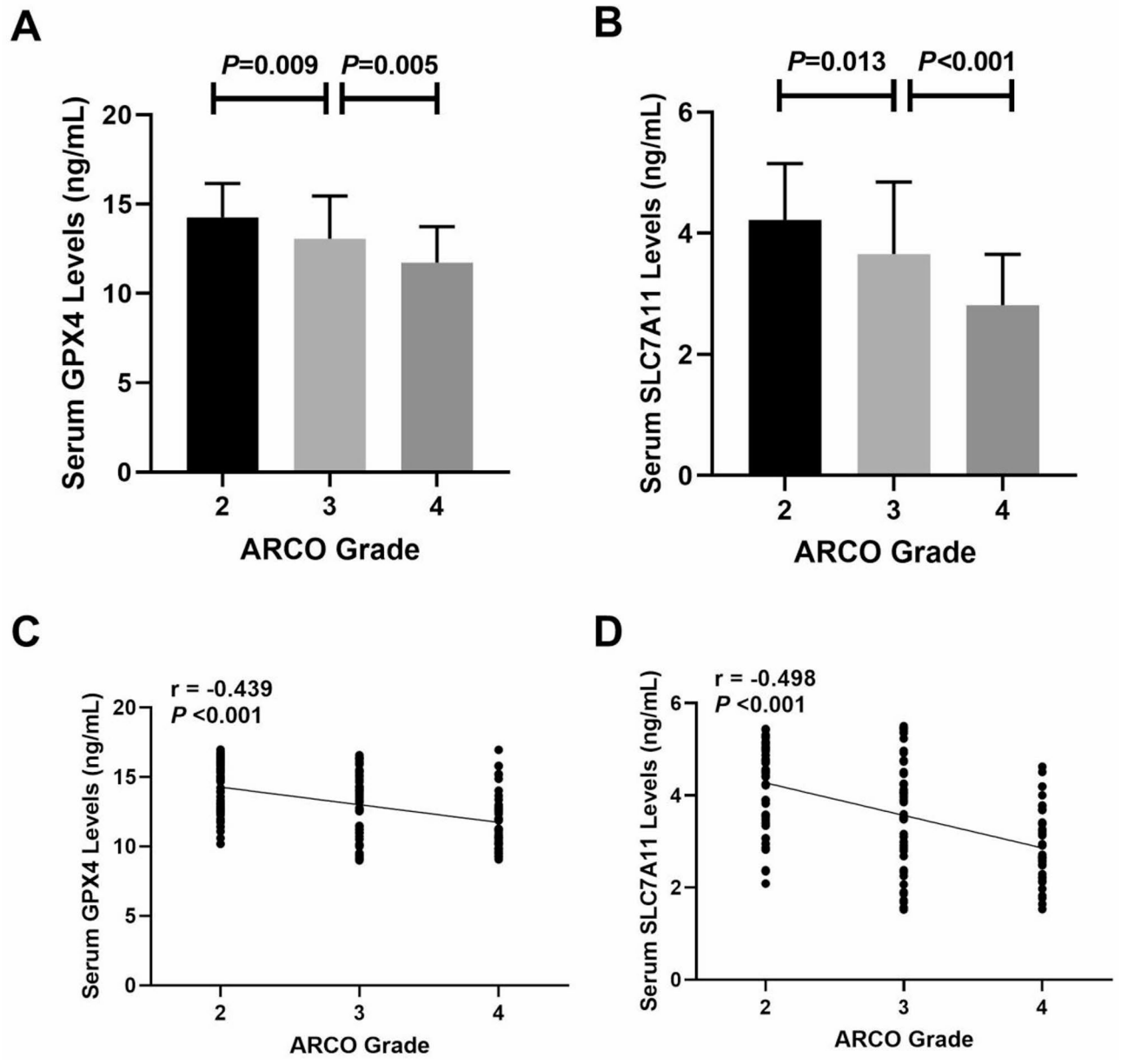

Fig. 5 (**A**) Comparison of serum GPX4 levels among ARCO stages; (**B**) Comparison of serum SLC7A11 levels among ARCO stages; (**C**) Relationship between serum GPX4 levels and different ARCO stages; (**D**) Relationship between SLC7A11 levels and different ARCO stages

and the activation of inflammatory signaling pathways, which in turn can increase the sensitivity of pain receptors and enhance the perception of pain [39]. The SLC7A11/GPX4 signaling pathway, by mitigating oxidative stress, can decrease the generation of inflammatory mediators like prostaglandins and interleukins, thereby significantly impacting pain sensation and its intensification [39]. The SLC7A11/GPX4 signaling pathway may offer relief from pain in diverse conditions, including low back pain, cancer-related pain, and inflammatory pain.

Our study had a few limitations. Firstly, this was a single-center study with limited sample size, and the majority of them were of Chinese descent. This limited the generalizability of our results to different ethnic groups. Future research should strive for larger, multicenter studies with diverse ethnic representations to validate the outcomes of this study. Secondly, our study is a cross-sectional study. Our findings did not reflect temporal changes in molecular markers, and the casual relationship between GPX4/ SLC7A11 and NT-ONFH was not clear.Therefore a longitudinal study is needed in the future. Thirdly, we did not observe the dynamic changes of GPX4 or SLC7A11 during disease progression and before or after treatment.Dynamic alternation of GPX4

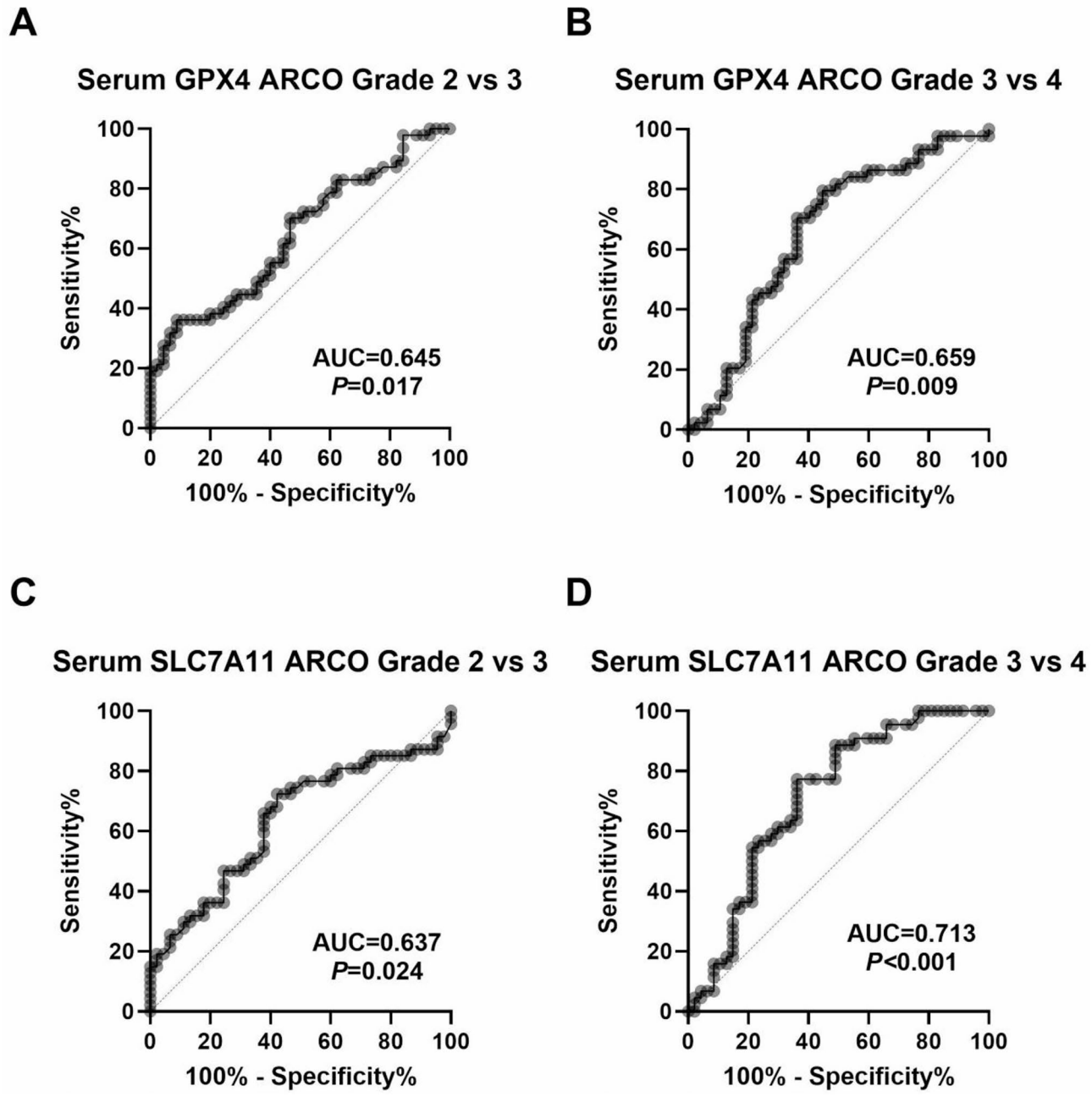

Fig. 6 (**A**) ROC curve assessment of serum GPX4 levels to differentiate between ARCO stage 2 and stage 3; (**B**) ROC curve assessment of serum GPX4 levels to differentiate between ARCO stage 3 and stage 4; (**C**) ROC curve assessment of serum SLC7A11 levels to differentiate between ARCO stage 2 and stage 3; (**D**) ROC curve assessment of serum SLC7A11levels to differentiate between ARCO stage 3 and stage 4

or SLC7A11 levels are need to be observed in the future. Fourthly, the molecular differences between steriod and alcoholic NT-ONFH were not deeply analyzed.Fifthly, while we concentrated on serum levels of SLC7A11 and GPX4, there are other ferroptosis-related markers that were not investigated, such as nuclear factor E2-related factor 2 (NRF2), and Ferrostatin-1. Examining these additional markers could provide further insights into the role of ferroptosis in osteonecrosis. Fifthly, our study was only an association study to evaluate SLC7A11 and GPX4 expression levels in the serum and local tissues of NT-ONFH patients. Deeper mechanistic experiments in vitro and in vivo including knockout/overexpressing cells or animal models to verify the specific pathways of GPX4/SLC7A11 regulating ferroptosis or targeting Iron-dependent cell death to alleviate pain or promote function activity are warranted in the near future.Further research is necessary to explore the potential applications and

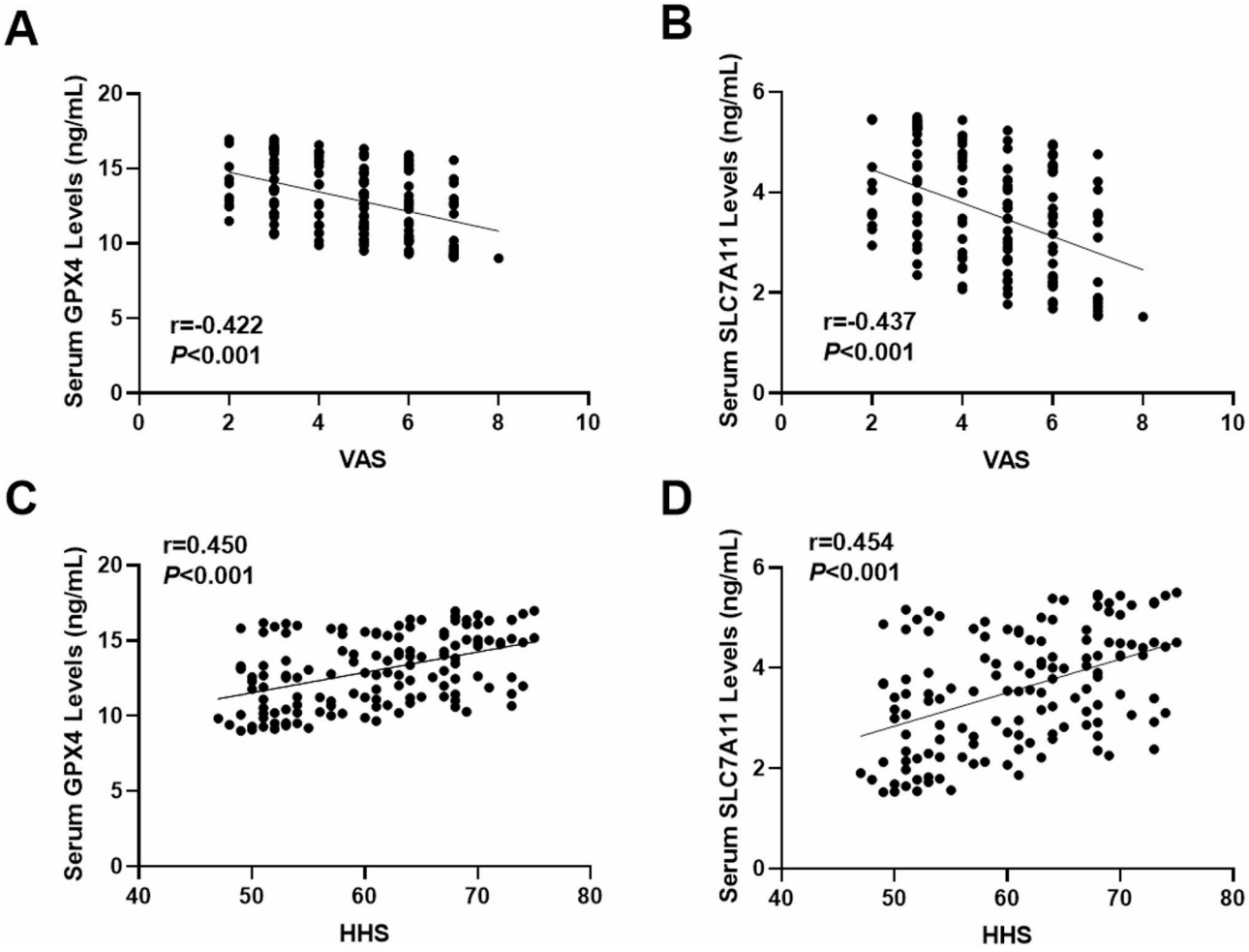

Fig. 7 (**A**) Correlation of serum GPX4 levels with VAS scores. (**B**) Correlation of serum SLC7A11 levels with VAS scores C.Correlation of serum GPX4 levels with HHS scores D.Correlation of serum SLC7A11 levels with HHS scores

mechanisms of these biomarkers in osteonecrosis, which could lead to a more thorough comprehension of the disease and possibly uncover new therapeutic approaches. Lastly, some confounders that may influence the expressions of SLC7A11 and GPX4 including comorbid medications use and other lifestyles like smoking history or physical activity were not fully considerated.

In conclusion, our study demonstrated that the reduction in both local and serum concentrations of SLC7A11 and GPX4 was correlated with the progression and severity of NT-ONFH, highlighting the significant part that ferroptosis plays in the evolution of this condition.

Acknowledgements
Not applicable.

Author contributions
YQH and WBF did clinical design, experiment work, data analyze and write the manuscript. YQH and ZP did experiment work and clinical work. ZYH, ZWX, ZHX and WB F did research design, manuscript review and project administration. All authors read and approved the final manuscript.

Funding
Not applicable.

Data availability
No datasets were generated or analysed during the current study.

Declarations

Ethics approval and consent to participate
This study was approved by Linyi People's hospital. All the patients signed written informed consent.

Consent for publication
Not applicable.

Competing interests
The authors declare no competing interests.

Author details
[1]Guangzhou University of Traditional Chinese Medicine, Guangzhou, Guangdong Province, China
[2]Linyi People's Hospital postgraduate training base of Guangzhou University of Traditional Chinese Medicine, Linyi, Shandong Province, China

Received: 25 March 2025 / Accepted: 11 May 2025

Published online: 17 May 2025

References

1. Migliorini F, Maffulli N, Baroncini A, et al. Prognostic factors in the management of osteonecrosis of the femoral head: A systematic review. Surgeon. 2023;21:85–98.
2. Quaranta M, Miranda L, Oliva F, et al. Osteotomies for avascular necrosis of the femoral head. Br Med Bull. 2021;137:98–111.
3. Migliorini F, Maffulli N, Eschweiler J, et al. Core decompression isolated or combined with bone marrow-derived cell therapies for femoral head osteonecrosis. Expert Opin Biol Ther. 2021;21:423–30.
4. Sadile F, Bernasconi A, Russo S, et al. Core decompression versus other joint preserving treatments for osteonecrosis of the femoral head: a meta-analysis. Br Med Bull. 2016;118:33–49.
5. Migliorini F, La Padula G, et al. Operative management of avascular necrosis of the femoral head in skeletally immature patients: A systematic review. Life (Basel). 2022;12:179.
6. Liu F, et al. An epidemiological study of etiology and clinical characteristics in patients with nontraumatic osteonecrosis of the femoral head. J Res Med Sci. 2017;22:15.
7. Zalavras C, et al. Potential aetiological factors concerning the development of osteonecrosis of the femoral head. Eur J Clin Invest. 2000;3:215–21.
8. Hines JT, Jo WL, Cui Q, et al. Osteonecrosis of the femoral head: an updated review of ARCO on pathogenesis, staging and treatment. J Korean Med Sci. 2021;36:e177.
9. Costa I, Barbosa DJ, Benfeito S, et al. Molecular mechanisms of ferroptosis and their involvement in brain diseases. Pharmacol Ther. 2023;244:108373.
10. Zhang C, Liu X, Jin S, et al. Ferroptosis in cancer therapy: a novel approach to reversing drug resistance. Mol Cancer. 2022;21:47.
11. Zhang J, Guo C. Current progress of ferroptosis in cardiovascular diseases. Front Cardiovasc Med. 2023;10:1259219.
12. Ratan RR. The chemical biology of ferroptosis in the central nervous system. Cell Chem Biol. 2020;27:479–98.
13. Chang S, Tang M, Zhang B, Xiang D, Li F. Ferroptosis in inflammatory arthritis: A promising future. Front Immunol. 2022;13:955069.
14. Sun CC, Xiao JL, Sun C, et al. Ferroptosis and its potential role in the physiopathology of skeletal muscle atrophy. Int J Mol Sci. 2024;25:12463.
15. Yang XD, Yang YY. Ferroptosis as a novel therapeutic target for diabetes and its complications. Front Endocrinol (Lausanne). 2022;13:853822.
16. Forcina GC, Dixon SJ. GPX4 at the crossroads of lipid homeostasis and ferroptosis. Proteomics. 2019;19:e1800311.
17. Yang WS, SriRamaratnam R, Welsch ME, et al. Regulation of ferroptotic cancer cell death by GPX4. Cell. 2014;156:317–31.
18. Ingold I, Berndt C, Schmitt S, et al. Selenium utilization by GPX4 is required to prevent hydroperoxide-induced ferroptosis. Cell. 2018;172:409.
19. Lin W, Wang C, Liu G, et al. SLC7A11/xCT in cancer: biological functions and therapeutic implications. Am J Cancer Res. 2020;10:3106–26.
20. Feng H, Stockwell BR. Unsolved mysteries: how does lipid peroxidation cause ferroptosis? PLoS Biol. 2018;16:e2006203.
21. Sun F, Zhou JL, Liu ZL, Jiang ZW, Peng H. Dexamethasone induces ferroptosis via P53/SLC7A11/GPX4 pathway in glucocorticoid-induced osteonecrosis of the femoral head. Biochem Biophys Res Commun. 2022;602:149–55.
22. von Mässenhausen A, Zamora Gonzalez N, Maremonti F, et al. Dexamethasone sensitizes to ferroptosis by glucocorticoid receptor-induced dipeptidase-1 expression and glutathione depletion. Sci Adv. 2022;8:eabl8920.
23. Zheng X, Ye FC, Sun T, et al. Delay the progression of glucocorticoid-induced osteoporosis: fraxin targets ferroptosis via the Nrf2/GPX4 pathway. Phytother Res. 2024;38:5203–24.
24. Xu L, Liu Y, Chen X, et al. Ferroptosis in life: to be or not to be. Biomed Pharmacother. 2023;159:114241.
25. Xue M, Tian Y, Sui Y, et al. Protective effect of fucoidan against iron overload and ferroptosis-induced liver injury in rats exposed to alcohol. Biomed Pharmacother. 2022;153:113402.
26. Yoon BH, Jones LC, Chen CH, et al. Etiologic classification criteria of ARCO on femoral head osteonecrosis part 1: glucocorticoid-associated osteonecrosis. J Arthroplasty. 2019;34:163–e1681.
27. Yoon BH, Jones LC, Chen CH, et al. Etiologic classification criteria of ARCO on femoral head osteonecrosis part 2: alcohol-associated osteonecrosis. J Arthroplasty. 2019;34:169–74.
28. Hawker GA, Mian S, Kendzerska T, et al. Measures of adult pain: visual analog scale for pain (VAS pain), Numeric Rating scale for pain (NRS pain), McGill pain Questionnaire (MPQ), Short-Form McGill pain Questionnaire (SF-MPQ), Chronic pain Grade scale (CPGS), Short Form-36 Bodily pain scale (SF-36 BPS), and Measure of Intermittent and Constant Osteoarthritis pain (ICOAP). Arthritis Care Res (Hoboken). 2011;63(Suppl 11):S240–52.
29. Nilsdotter A, Bremander A. Measures of hip function and symptoms: Harris hip score (HHS), hip disability and osteoarthritis outcome score (HOOS), Oxford hip score (OHS), Lequesne index of severity for osteoarthritis of the hip (LISOH), and American academy of orthopedic surgeons (AAOS) hip and knee questionnaire. Arthritis Care Res (Hoboken). 2011;63(Suppl 11):S200–7.
30. Chen N, Meng Y, Zhan H, et al. Identification and validation of potential ferroptosis-related genes in glucocorticoid-induced osteonecrosis of the femoral head. Med (Kaunas). 2023;59:297.
31. Miao Y, Chen Y, Xue F, et al. Contribution of ferroptosis and GPX4's dual functions to osteoarthritis progression. EBioMedicine. 2022;76:103847.
32. Sheng W, Liao S, Wang D, Liu P, Zeng H. The role of ferroptosis in osteoarthritis: progress and prospects. Biochem Biophys Res Commun. 2024;733:150683.
33. Liu P, Wang W, Li Z, et al. Ferroptosis: A new regulatory mechanism in osteoporosis. Oxid Med Cell Longev. 2022;2022:2634431.
34. Gao Z, Chen Z, Xiong Z, et al. Ferroptosis - A new target of osteoporosis. Exp Gerontol. 2022;165:111836.
35. Deng X, Lin B, Wang F, et al. Mangiferin attenuates osteoporosis by inhibiting osteoblastic ferroptosis through Keap1/Nrf2/SLC7A11/GPX4 pathway. Phytomedicine. 2024;124:155282.
36. Fan S, Wang K, Zhang T, et al. Mechanisms and therapeutic potential of GPX4 in pain modulation. pain ther. Published Online November. 2024;6. https://doi.org/10.1007/s40122-024-00673-8.
37. Zhang Y, Si W, Mao Y, et al. Upregulation of ferroptosis in glucocorticoids-induced posterior subcapsular cataracts. Commun Biol. 2025;8(1):613.
38. Li C, Zhou S, Chen C, et al. DDTC-Cu(I) based metal-organic framework (MOF) for targeted melanoma therapy by inducing SLC7A11/GPX4-mediated ferroptosis. Colloids Surf B Biointerfaces. 2023;225:113253.
39. Li L, Guo L, Gao R, et al. Ferroptosis: a new regulatory mechanism in neuropathic pain. Front Aging Neurosci. 2023;15:1206851.

Publisher's note